Earthquake Geotechnical Engineering for Protection and Development of Environment and Constructions – Silvestri & Moraci (Eds)
© 2019 Associazione Geotecnica Italiana, Rome, Italy, ISBN 978-0-367-14328-2

The use of numerical analysis in the interpretation of liquefaction case histories

S.L. Kramer
University of Washington, Seattle, WA, USA

M.W. Greenfield
Greenfield Geotechnical, Portland, OR, USA

ABSTRACT: The development of improved, validated constitutive models for liquefiable soils, and their implementation into nonlinear, effective stress ground response analyses, can be used to beneficially augment the interpretation of liquefaction triggering case histories. The availability of subsurface data, collected either before or after an earthquake that causes liquefaction, allows the development of site models that can help identify the critical layer(s) and understand the interaction of various soil layers that control the system response of the soil profile. The benefits of such analyses depend on the ability of the numerical analysis to capture important elements of liquefiable soil behavior, and on the ability to approximate the input motions that produce the observed liquefaction. The main issues involved in these analyses are discussed and the use and benefits of numerical analyses illustrated with a case history from the 2011 Tohoku earthquake in which an initial interpretation of liquefaction at shallow depth has been shown to be much less likely than liquefaction of a deep (approximately 17 m) layer of soil.

1 INTRODUCTION

Evaluation of liquefaction hazards has relied, for the past 40+ years, on empirical procedures rooted in case histories. Case histories have been crucial in the development of useful empirical procedures, but also in giving engineers and the public a view of the importance of liquefaction and the type of damage that it can cause to buildings, bridges, dams, pipelines, and other elements of infrastructure. Well-documented case histories include accurate characterization of subsurface geometry including groundwater levels, accurate measurement or estimation of ground motions, accurate representation of material properties including soil plasticity, density, stiffness, and depositional history, and detailed interpretation of all of these factors to identify the characteristics of the case history that inform appropriate empirical models.

In recent years, numerical analyses and the constitutive models embedded within them have improved to the point where they can provide reliable indications of the general behavior of soil profiles with potentially liquefiable layers under earthquake shaking. Constitutive models that account for important soil behavioral phenomena before, during, and after triggering of liquefaction are now available, and have been implemented into dynamic analyses that are accessible to researchers and, increasingly, practitioners. This paper describes such analyses and explores the manner in which they can be used in the interpretation and analysis of liquefaction case histories.

2 LIQUEFACTION

The importance of soil liquefaction is well established, as it has been demonstrated over and over in historical and recent earthquakes. Liquefiable soils exist in many highly populated coastal areas which are developed with constructed facilities such as ports and bridges that support commerce and local/regional economies. The ground deformations associated with liquefaction have caused tremendous damage and losses to such facilities in recent earthquakes, indicating that further progress remains to be made in both the evaluation and mitigation of liquefaction hazards. Liquefaction hazard evaluations generally include three primary components – evaluation of liquefaction susceptibility, assessment of the potential for triggering of liquefaction in susceptible soils, and prediction of the effects of liquefaction if and when triggered.

2.1 *Susceptibility*

Not all soils are susceptible to liquefaction, and susceptibility has been correlated primarily to soil plasticity. Soils with fines of significant plasticity tend to be less contractive than non-plastic soils and hence generate less pore pressure under cyclic loading of a given amplitude and duration. Different investigators have interpreted laboratory and field data differently in terms of plasticity index (PI) ranges corresponding to susceptible and non-susceptible behavior. Boulanger and Idriss (2006) considered soils to exhibit sand-like (liquefaction susceptible) at PI values less than 3 and clay-like (not susceptible) behavior at PI values greater than 8. The range of $3 < PI < 8$ was interpreted as a transition zone and a value of $PI = 7$ was recommended as an appropriately conservative deterministic "boundary." Bray and Sancio (2006) considered soils with $PI < 12$ and a ratio of water content (wc) to liquid limit (LL) of $wc/LL > 0.85$ to be susceptible to liquefaction, soils with $PI > 20$ or $wc/LL < 0.80$ to be non-susceptible, and soils with other combinations of PI and wc/LL to be potentially susceptible. Because the water content of a saturated soil is an indicator of density, the wc/LL ratio may be considered to be part of the triggering issue rather than one of pure susceptibility. Nevertheless, both procedures agree that soils with very low plasticity ($PI < 7$) should be considered susceptible to liquefaction, soils with high plasticity ($PI > 20$) should be considered non-susceptible, and soils with intermediate plasticity should be sampled and tested in the laboratory to determine their pore pressure generation and stress-strain behavior.

2.2 *Triggering*

Liquefaction is triggered by the generation of excess pore pressure and consequent softening of the soil under reduced effective stresses. The actual point of triggering, however, is defined in different ways both in the laboratory and in the field. The classic definition of liquefaction was that of "initial liquefaction," i.e., the generation of excess pore pressure in laboratory tests equal to the initial effective stress, defined as a pore pressure ratio, $ru = 100\%$. Alternative laboratory definitions were developed for soils that may exhibit significant softening without actually reaching a state of initial liquefaction; such definitions are typically based on strain amplitude thresholds, e.g., shear strain, $\gamma > +/- 3\%$. Since loading can be controlled and response measured accurately in the laboratory, such definitions of the triggering of liquefaction, although different from each other, are quite useful. In the field, however, instruments for measuring ground motions, pore pressures, deformations, etc. at liquefiable sites are extremely rare. The triggering of liquefaction in the field is nearly always interpreted from surficial evidence such as the presence (or absence) of sand boils, ground cracking, etc.

Surficial evidence develops when high pore pressures in a layer of thickness sufficient to expel a large volume of water that is overlain by a non-liquefied crust that is sufficiently thin to allow water to travel quickly enough to the surface to entrain liquefied and overlying soils to produce piles of ejecta on the surface. Thus, initial liquefaction likely occurs at some depth in the ground before surficial evidence is produced. It should be noted that a thin layer of

sand may liquefy beneath a thick crust and not expel enough water to produce surficial evidence, and a thick layer of sand overlain by a thin crust may develop pore pressures that approach, but do not reach, initial liquefaction, can still cause hydraulic gradients sufficient to produce surficial features normally taken as evidence of liquefaction. Thus, there is a potential for surficial evidence to serve as false positive or false negative indications of liquefaction.

2.3 *Effects*

Its damaging effects are what make liquefaction such an important part of geotechnical earthquake engineering practice. The effects of liquefaction can range from scattered sand boils involving relatively small volumes of soil up to massive flow slides. Often, the most visible effect of liquefaction and, as previously described, a frequent criterion for classification of liquefaction/non-liquefaction case histories, is the presence/absence of sand boils. While sand boils themselves are not particularly damaging, the volume of ejecta they contain is removed from below the original ground surface and can cause, in extreme cases, significant settlement of the original ground surface.

While flow slides occur only rarely, smaller ground failures such as lateral spreads occur much more frequently and cause much more damage to infrastructure and constructed facilities. Lateral spreads involve both lateral and vertical deformations that can impose large deformation demands on structures supported by shallow foundations, and large kinematic demands on the types of deep foundations frequently used to support structures underlain by liquefiable soils. Liquefaction can also lead to settlement, both in the free-field and in the vicinity of structures. Free-field settlement results from dissipation of excess pore pressures generated during earthquake shaking and from additional compressibility resulting from alteration of the soil fabric by post-triggering shear straining. Additional settlement can occur near structures supported on shallow foundations as locally higher shear stresses are induced in the soil by the dynamic response of the structure itself.

The triggering of liquefaction can also affect the nature of ground motions. The softening of a soil profile over the duration of a ground motion can lead to changes in the frequency content of the motion transmitted to the ground surface. Prior to triggering, a soil profile containing potentially liquefiable soils will generally be stiff enough to transmit high-frequency ground motions to the surface. After triggering, however, the stiffness of the soil may drop to levels that cause higher frequency components of a motion to be reflected back downward by the impedance contrast that develops at the bottom of the softened layer. The result is a transition, often sharp, from high-frequency to low-frequency surface motions at the time of liquefaction. The nature of that transition depends on many factors including the density and thickness of the liquefiable layers and the characteristics of the ground motion.

3 CASE HISTORIES

As previously indicated, case histories are critical to the development of empirical procedures for liquefaction hazard evaluation. Case histories have historically been developed by individual investigators or small teams of investigators operating independently and with different protocols. Over the past 20 years, case history documentation has been advanced considerably by the formation of the Geotechnical Extreme Events Reconnaissance (GEER) association and the increased availability of useful tools such as digital cameras, GPS, LiDAR, and other forms of remote sensing. Current efforts of the Next Generation Liquefaction (NGL) project (Stewart et al., 2016) are providing guidance for more complete and consistent documentation and dissemination of liquefaction case history data.

3.1 *Characterization*

Development of a complete and useful case history requires documentation of field performance, characterization of geotechnical conditions, and measurement or estimation of

loading in the form of ground motion intensity measures. A well-documented case history will include the precise location of the site, descriptions of ground failure (or lack thereof) at and near the site, and the date/time of the observations. Ground failure descriptions will ideally be supplemented by photographs (from land and/or unmanned aerial vehicle (UAV)), maps of observed features, and available advanced imaging such as LiDAR and aerial/satellite imagery. Geotechnical conditions will include soil stratigraphy, depositional environment including age, groundwater conditions, soil types including gradation parameters and plasticity characteristics, water contents, shear wave velocities, penetration resistances, and other data. Ground motion intensity measures are needed as descriptors of loading at liquefaction case history sites. Because ground motions are only rarely recorded at liquefaction case history sites, intensity measures must usually be estimated, and a number of approaches of varying complexity and accuracy can be used. If the earthquake that produced the case history is in the ground motion database used to construct a modern ground motion prediction equation (GMPE), the IM can be estimated as the sum (in natural log units) of the median predicted IM, the event term associated with that earthquake for the GMPE, and a within-event residual that accounts for spatial correlations in path and source (e.g., Bradley, 2014; Kwak et al., 2015). If relatively nearby recordings are available but the event was not part of the GMPE, the aforementioned procedure can be used with the event term set to zero. If nearby recordings are not available but a ShakeMap is, the ShakeMap IM values can be used. If none of the preceding are available, median GMPE values can be used.

3.2 *Documentation*

As previously noted, early case history databases were developed by individual researchers and generally closely held by those researchers who often had invested considerable time and expense to their acquisition and who had the type of detailed knowledge of the case histories that was required for their proper interpretation. Over time, case history data has become more widely available, at least in the form of data summaries or metadata, often presented in flatfiles. Such flatfiles include both objective and subjective data, with the subjective data including judgment and interpretations made by the person or group that developed the database. The case history database being compiled by the NGL project is different in that it is objective with factual information on field performance, geotechnical conditions, and ground motions.

3.3 *Interpretation*

Parameterization of case history data for the purpose of empirical model development generally requires interpretation of that data in order to fit within the simplified framework of a practical empirical model. Case history issues that require interpretation include determination of whether liquefaction was or was not triggered, identification of the "critical layer" that liquefied, characterizing the significant properties of that critical layer, and characterizing the loading, or seismic demand, imposed on the critical layer. Because many of these issues rely on measurements either not made or made after an earthquake has occurred, their resolution must be based on interpretations that have moderate to high levels of subjectivity. In past cases, different interpretations by different researchers have led to inconsistencies in empirical predictive models.

Among the most critical, and often difficult, interpretations are those associated with the critical layer. In fact, the actual existence of a critical layer is a matter of some discussion – the notion that the response of a liquefied soil profile can be characterized by the properties of a single layer, rather than the characteristics of the entire soil profile that acts as a "system," is somewhat unclear. Nevertheless, the concept of a critical layer underlies all existing empirical triggering models. The critical layer in liquefaction case histories is usually taken as the "weakest-link" layer, usually interpreted as the layer with the highest

liquefaction potential (i.e., lowest factor of safety against triggering). That layer would be expected to be the layer that liquefied first in a soil profile in which more than one layer actually liquefied. Criteria developed as part of paleoliquefaction investigations have helped define best practices for critical layer identification, but considerable judgment is still required to apply them.

Once the critical layer has been identified, it must be characterized by a single, "representative" penetration resistance value. This can be difficult in layers with variable resistances, particularly when high-resolution CPT data is used. Some investigators have taken the lowest penetration resistance as the representative value, and others have taken the average penetration resistance over the layer thickness. In the latter case, critical layer thickness can be an issue that requires application of judgment. However, numerical analyses can be used to assist in the averaging process. By assuming different penetration resistances that are held constant over the thickness of the representative layer, computed values of some metric of liquefaction occurrence (time of liquefaction, intensity measure amplitude, etc.) can be compared with values computed for the actual variable profile of penetration resistance over the thickness of that layer to identify the constant value that produces a response that matches that produced by the variable values.

The loading imposed on the critical layer must also be determined in order to completely characterize the case history. The loading is usually characterized by the cyclic stress ratio, CSR, which is characterized as a function of the peak ground surface acceleration and the magnitude of the causative earthquake in the simplified method. The CSR can also be computed by means of site-specific ground response analyses; the analyses must be performed as total stress analyses since the effects of pore pressure generation are assumed not to be included in current procedures.

4 AN EXAMPLE – IBR014

IBR014 is a K-Net strong motion recording station located about 60 km north of Tokyo in the city of Tsuchiura on the west side of Kasumigaura Lake (Figure 1). The recording station was originally established as a standard K-Net site in 1996 and has been upgraded several times, most recently to a K-NET11A instrument in 2014. The instrument rests within a small protected enclosure on a stiff spread footing resting on the ground surface.

Figure 1. Location of IBR014 strong motion station and aerial view of site following earthquake. Note location of ejected sand in lower parking lot and lack of ejecta in upper parking lot and area surrounding instrument.

4.1 *Site conditions*

The recording station was in a parking lot on the side of a terrace approximately 8 m above and 375 m south of the Sakura River which flows into Kasumigaura Lake. The ground rises at an approximately 3:1 (H:V) slope to the west of the parking lot and slopes downward more gradually (approximately 30:1) to the east. A three-story building is located about 5 m south of the IBR014 instrument. The parking lot is divided into two sections – an upper parking lot that lies to the west and north of a smaller, lower parking lot that abuts the west side of the building; the two sections are separated by a small (0.3 m) wall. Another short wall separates the lower parking lot from a parking area immediately in front (south) of the three-story building. These parking areas appear to be part of a series of shallow terraced cuts and fills that follow the natural grade of the hillside to the south and east of the IBR014 site.

4.2 *Ground motions*

The IBR014 instrument recorded strong shaking during the Tohoku earthquake. Peak ground accelerations were 0.51 and 0.39 in the EW and NS directions, respectively; peak ground velocities were 0.34 and 0.26 m/sec in those directions. The significant duration (T5-95) was over 70 sec. The recorded time histories are shown in Figure 2. The acceleration amplitudes increased slowly until about 110 sec when the peak acceleration was reached in the EW direction. Shortly after that, the acceleration amplitude decreased and the frequency content of the two horizontal components appeared to shift toward lower frequencies.

A Stockwell transform (Stockwell et al., 1996) was used to examine the temporal variation of frequency content. Figure 3 shows a normalized Stockwell power spectrogram that shows the evolving amplitude-normalized (in order to better illustrate the frequency content of the lower amplitude portions of the record) frequency content of the recorded horizontal motions. The spectrogram shows that the early (albeit very weak) portion of the record has a dominant frequency of about 10 Hz. As the amplitude of shaking increases, the dominant frequency slowly decreases to 7-8 Hz at about 100 sec. Shortly after that time, the dominant frequency drops quite rapidly to about 1 Hz with a near absence of motions greater than 2-3 Hz. This rapid drop in frequency, which was observed in both horizontal components but not the vertical component, is an indication of the triggering of liquefaction (Kramer et al., 2016) at a time of approximately 110 sec. The time history after 110 sec is characterized by low frequency motion intermittently interrupted with higher-frequency spikes likely caused by strong dilation-induced stiffening of the profile.

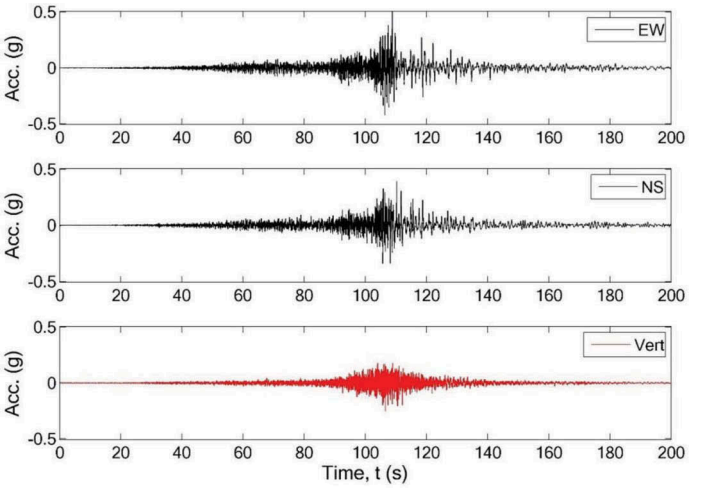

Figure 2. Recorded ground surface motions at IBR014 site in 2011 Tohoku earthquake.

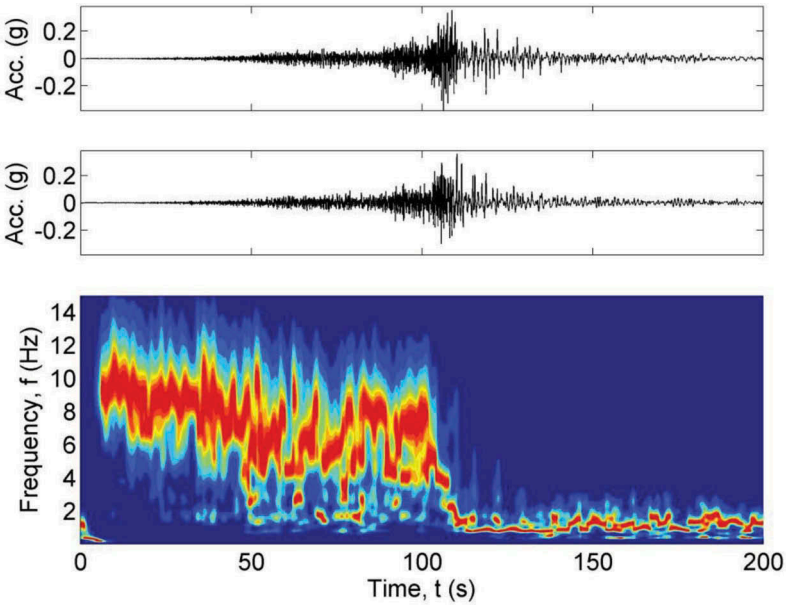

Figure 3. Horizontal ground surface time histories and normalized Stockwell spectrogram for IBR014 ground surface motion.

4.3 *Observations*

Surficial evidence of liquefaction was observed near IBR014 during the GEER reconnaissance after the Tohoku earthquake (Ashford et al., 2011). Ejecta was observed in the lower parking lot but, even though its pavement was cracked, not in the upper parking lot. Reconnaissance notes indicated that the small retaining wall between the lower parking lot and the three-story building parking area appeared to have failed by tilting. The cracked pavement in the upper parking lot suggests that shaking was strong enough to produce some permanent deformation of the shallow soils beneath it. The lack of ejecta in that area, despite the existence of cracks that would have allowed liquefied soil to easily be ejected, suggests that shallow soils beneath the upper parking lot did not liquefy.

4.4 *Subsurface conditions*

A 20 m boring drilled during installation of the IBR014 instrument showed a relatively simple profile consisting of about 1 m of fill underlain by 3.7 m of sand, 12.6 m of silt, and then sand to the depth of the exploration. SPT resistances ranged from 1 to 11 blows/ft in the upper sand layer and 13-33 blows/ft in the lower sand layer. Shear wave velocities were 90-190 m/sec in the upper sand and about 420 m/sec in the lower sand. The measured p-wave velocity increased from 500 to 900 m/s at a depth of 1 m without an increase in s-wave velocity. The p-wave velocity then increased again to about 1,470 m/s at a depth of 8 m within the silt layer. The fact that this velocity is close to the p-wave velocity of water suggests that the ground-water level at the site could have been at about 8 m depth at the time the instrument was installed.

A supplemental subsurface investigation was conducted by the University of Washington and Tokyo Soil Research in September, 2015. The investigation took place after a prolonged period of intense rainfall, and standing water and wet spots were observed on the west side of the parking lot. The supplemental investigation included a mud rotary boring to a depth of 30.3 m, a cone penetration test (CPT) probe to a depth of 27.2 m and seismic cone shear and p-wave velocity measurements. Pilot holes for both the boring and the CPT probe were

hand-augured to a depth of about 2 m before drilling and probing to collect grab samples. Groundwater was encountered at a depth of about 1.3 m in the pilot holes. The hydrostatic pore pressure was measured with the CPT piezometer after excess pore pressure dissipated, and the piezometric surface of the groundwater was about 1.3 m deep at the time of the investigation. The difference in recorded groundwater depths, along with weather observations, suggest that groundwater levels at the site are variable and likely influenced by drainage from the hillside to the west of the site. Fluctuating groundwater levels can preclude complete saturation of soils within zones of fluctuation.

The soil profile interpreted from the supplemental subsurface investigation is shown in Figure 4. The upper material characterized as sand in the K-Net boring consisted of 6 m of clay and clayey sand, which was indicated by the locally-based drilling contractor to be prevalent in the Tsuchiura area. That layer was underlain by about 9 m of silt, which was in turn underlain by an alternating sequence of sand, silty sand, and sandy silt to the depth explored. Shear wave velocities were in the range of 200-300 m/sec. Corrected SPT resistances were variable, ranging from about 12-20 blows/ft in the upper sandy layers and 12-22 in the lower sandy layers. CPT tip resistances were generally consistent with the SPT resistances, being higher in the sandy layers and lower in the silty layers. The CPT Soil Behavior Type Index, I_c, varied from about 2 to 5 with values generally below 2.5 in the shallow clayey sand and above 3 in the silty materials.

The shallow clayey sand materials at 2-6 m depth had fines contents ranging from 33-39% and plasticity indices of 17-22. Shear wave velocities of the clayey sand and sandy clay ranged from about 200-260 m/sec. The silt layer was soft at 7 m depth and transitioned to medium stiff to stiff below a depth of 8 m. The silt contained 22-43% sand-sized particles and had a plasticity index of about 20. The shear wave velocity of the silt ranged from about 160-280 m/sec. The lower sand layers, which were themselves non-plastic but interbedded with sandy silt below about 17 m depth, were medium dense to dense with shear wave velocities ranging from about 220-400 m/sec.

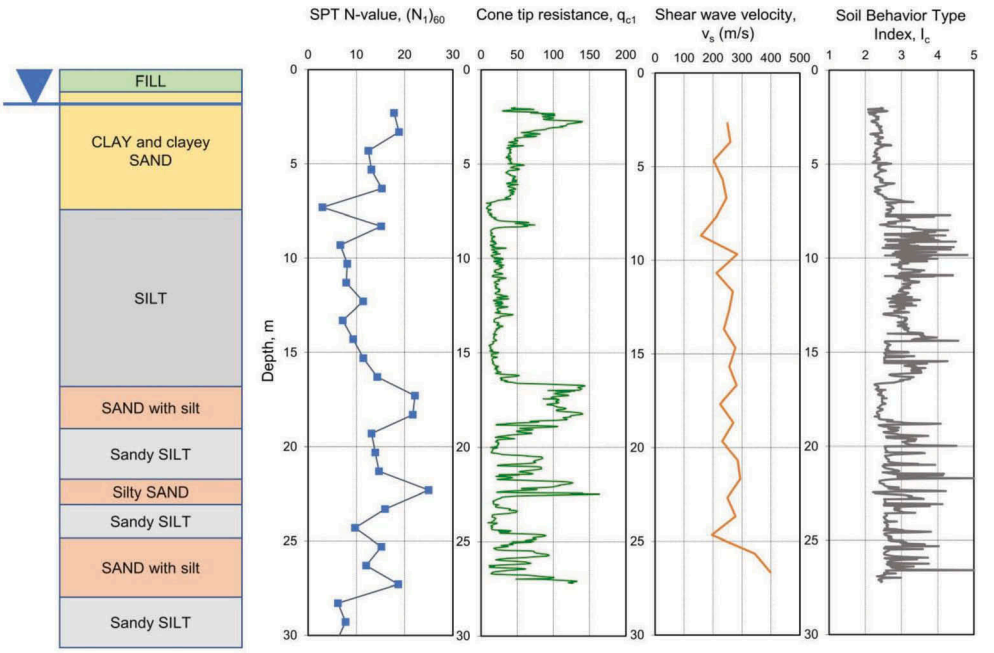

Figure 4. Soil profile with accompanying profiles of SPT resistance, CPT tip resistance, shear wave velocity, and soil behavior type index from the IBR014 supplementary subsurface investigation.

5 INTERPRETATION OF IBR014 CASE HISTORY

Interpretation of the IBR014 case history requires resolution of a number of complicating and potentially conflicting aspects of the site conditions and observations following the Tohoku earthquake. These include:

1. The liquefaction observations were made at some distance from the strong motion instrument. Surficial evidence was not found immediately adjacent to the instrument even though cracks in the upper parking lot pavement would have allowed easy transmission of ejecta from a shallow liquefied layer to the surface. Instead, only a modest amount of liquefaction ejecta was observed in the lower parking lot, which may have been constructed on a thin layer of fill to terrace the ground surface over the gently sloping natural terrain.
2. The groundwater level at the time of the earthquake is not known. The groundwater was 1.3 m deep when the supplemental subsurface investigation took place after a period of heavy, sustained rainfall. However, based on the results of the p-wave velocities measured by the National Research Institute for Earth Science and Disaster Resilience (NIED), the groundwater level could have been as deep as 8 m at the time of the earthquake. Fluctuations of groundwater levels are not uncommon and are known to result in partially saturated conditions within the zone of moisture change; the indicated difference in groundwater levels could be quite large at the IBR014 site. However, based on the presence of ejecta in the lower parking lot near the site, the groundwater was likely relatively shallow during the earthquake.
3. Strong evidence of liquefaction was observed in the ground surface recording. Both horizontal components of ground motion were observed to undergo a strong and sudden shift in frequency content toward very low frequencies at about 104-110 sec, and dilation-induced acceleration pulses were observed to be superimposed on the low-frequency motion after 110 sec. The change in frequency content was not observed in the vertical component of motion.
4. The plasticity of the shallow clayey sands was high enough to render them clearly non-susceptible according to the Boulanger and Idriss (2006) criterion. That plasticity level, along with water contents approximately equal to their liquid limits, gives them a rating of borderline non-susceptible according to the Bray and Sancio (2006) criterion.
5. The shallow clayey soils were prevalent in the Tsuchiura area but were not observed to have liquefied at other locations.
6. The deeper sand layers were non-plastic and hence highly susceptible to liquefaction.

5.1 *Empirical triggering analyses*

A series of empirical triggering analyses were performed for the IBR014 soil profile. Although the ground surface motion was recorded at the site, the record was influenced by pore pressure generation and the triggering of liquefaction, so its peak acceleration was inconsistent with the definition of peak acceleration used in empirical liquefaction triggering analyses. In order to estimate the most appropriate peak acceleration value to use in the empirical analyses, the values that would have been recorded at the IBR014 site had liquefaction not occurred had to be estimated. This estimate was made using the BCHydro (Abrahamson et al., 2016) ground motion prediction equation (GMPE) along with four recorded motions from instruments located near the IBR014 station (data from three other nearby instruments were not used because of instrument failure, excessive topographic effects, and a Vs30 value that was below the minimum for the BCHydro GMPE). The recorded motions used in this process were from the IBR011, IBR012, IBR017, and IBRH17 instruments that essentially surround the IBR014 site; characteristics of those motions and their sites are summarized in Table 1. The sites are similar distances from the rupture surface, relatively close to IBR014, have similar Vs30 values, and recorded similar ground motion intensities and durations.

Table 1. Characteristics of IBR014 and nearby surrounding sites.

Station	R_{rup} (km)	Distance from IBR014 (km)	V_{s30} (m/sec)	Geomean PGA (g)	Arias Intensity (m/sec)	$T_{5\text{-}95}$ (sec)	Observations
IBR014	71	0	270	0.45	4.6	68.2	Liquefied
IBR011	81	11	240	0.35	4.5	54.3	No liquefaction
IBR012	64	15	190	0.30	4.6	68.3	No liquefaction
IBR017	59	17	260	0.42	4.7	51.9	No liquefaction
IBRH17	60	11	300	0.40	5.9	48.3	No liquefaction

The Tohoku earthquake was determined to have an event term of 0.14 for 0.01-sec spectral acceleration in the BCHydro GMPE, so that term was added to the (ln) median to obtain an event-specific estimate of PGA at the IBR014 site. It was also noted that individual ground motions in the vicinity of Tsuchiura could have deviated from the event-specific median PGA value due to regional factors or factors that were not included in the source, path, site, or event terms in the GMPE. Regional residuals were calculated using inverse distance-weighted interpolation from the four ground motions near the IBR014 station after correcting for differences in site distance and V_{s30} value. Application of these residuals led to an adjusted estimated geometric mean peak acceleration of 0.35 g, which was close to the highest acceleration (0.34 g) that had been recorded at IBR014 before triggering, but significantly lower than the recorded PGA of 0.45 g.

Using the estimated PGA with the actual magnitude of the Tohoku event, factor of safety values were computed based on both SPT and CPT resistances using the Idriss and Boulanger (2014) empirical triggering procedure. Figure 5(a) shows the computed factors of safety assuming the shallow (< 7 m depth) sandy materials are both susceptible to liquefaction and completely saturated, and Figure 5(b) shows factor of safety profiles assuming those soils are not susceptible. The shallow sandy soils show extremely low factors of safety for both SPT and CPT procedures, particularly at depths of 3-7 m. The potential effects of liquefaction can be expressed in terms of liquefaction severity indices. The value of liquefaction potential index, LPI (Iwasaki et al, 1978), Ishihara-inspired liquefaction potential index, LPI_{Ish} (Maurer

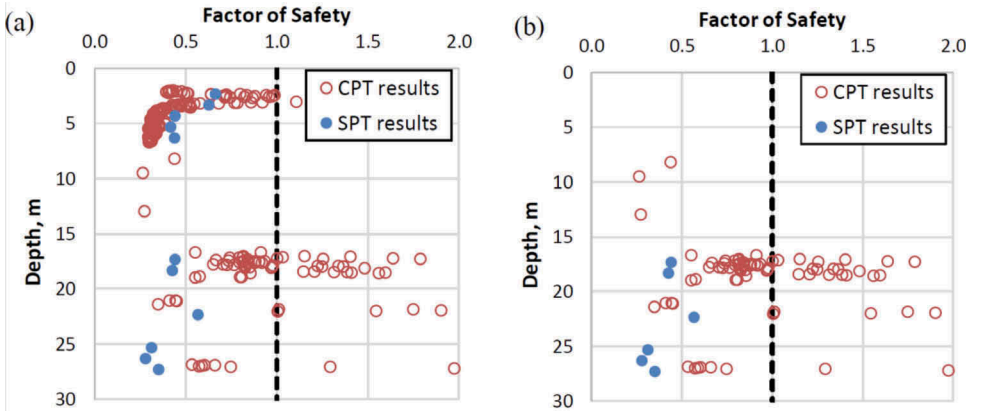

Figure 5. Variation of empirical factor of safety against liquefaction triggering with depth: (a) assuming shallow sandy soils are susceptible to liquefaction and fully saturated, and (b) assuming shallow sandy soils are non-susceptible or unsaturated.

Table 2. Liquefaction severity index parameters and implied performance for cases in which shallow sandy soils are assumed to be susceptible and non-susceptible to liquefaction.

Severity Index Parameter	Susceptible	Non-Susceptible
LPI	26.7 (very high risk of significant surficial evidence)	0.3 (low risk of significant surficial evidence)
LPI_{Ish}	22.2 (very high risk of significant surficial evidence)	0.0 (very low risk of significant surficial evidence)
LSN	42.7 (Major expression of liquefaction)	0.73 (Little or no expression of liquefaction)
Reconsolidation settlement	20 cm	1 cm

et al., 2015), and liquefaction severity number, LSN (van Ballagooy et al., 2013) were computed assuming the shallow sandy materials are susceptible and non-susceptible to liquefaction. Table 2 shows the results of these analyses, which all indicate that the observed performance of the IBR014 site was much more consistent with the expected performance if the shallow sandy materials were not susceptible to liquefaction than if they were.

5.2 *Numerical analyses*

In order to gain additional insight into the nature of the IBR014 profile response, a series of nonlinear, effective stress site response analyses were performed with the computer program, FLIP (FLIP Consortium, 2011). The previously described procedure for evaluating the non-liquefied PGA at the site was repeated for all spectral periods to develop an estimated non-liquefied target spectrum. The adjusted (for distance and V_{s30}) spectra from the four nearby stations and inverse-distance-weighted IBR014 target spectrum are shown in Figure 6(a). The four spectra can be seen to be generally consistent with each other and with the target spectrum. Following establishment of the target spectrum, over 1,500 motions from Tohoku and several other very large magnitude earthquakes were compared with the target spectrum and with the significant durations of the nearby recorded motions. A suite of 11 linearly-scaled motions that best fit the target spectrum with significant durations close to those from the nearby records was developed; spectra for the selected motions are shown in Figure 6(b). The scaling factors used to optimize the fit to the target spectrum are provided in Table 3.

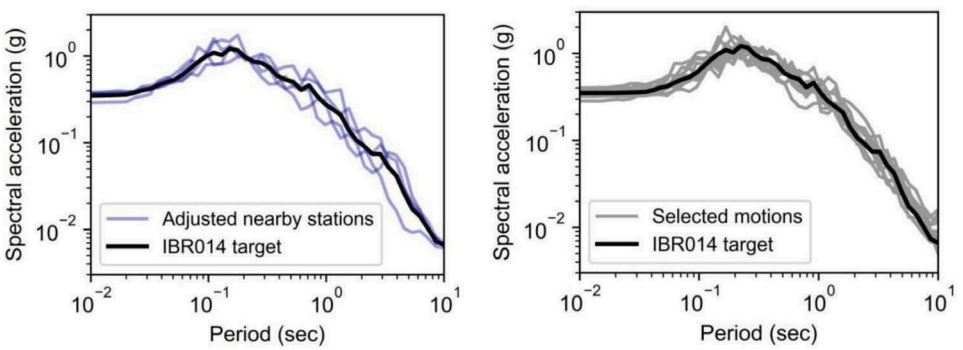

Figure 6. Response spectra for non-liquefied profile at IBR014 site: (a) adjusted nearby stations and interpolated IBR014 target spectrum, and (b) IBR014 target spectrum and spectra from 11scaled motions.

Table 3. Selected ground motions that best fit the target spectrum for IBR014.

Earthquake	Station	Scaling factor
Tohoku	IWT011E-W	0.95
Tohoku	YMT007N-S	1.81
Tohoku	IBR008E-W	1.09
Tohoku	FKS015E-W	1.71
Tohoku	IWT021E-W	1.11
Tohoku	IWT021N-S	1.20
Tohoku	TCH001E-W	0.95
Tohoku	IWTH204	0.87
Tohoku	IWTH105	0.64
Tohoku	AING174	2.59
Tohoku	IWT026N-S	0.89

The FLIP analyses were performed using the Cocktail glass model (Iai et al., 2011) to represent potentially liquefiable soils layers. The Cocktail glass model can account for pore pressure generation, phase transformation behavior approaching and following triggering of liquefaction, and fabric degradation that can occur after triggering. The Cocktail glass model was calibrated to produce pore pressure generation and stress-strain behavior consistent with that observed in the laboratory and with that inferred from case history-based empirical procedures for evaluation of liquefaction potential. Specifically, the calibration sought to match the empirical triggering relationship of Boulanger and Idriss (2014) with rates of pore pressure generation consistent with laboratory data reported by De Alba et al. (1976) and strain levels consistent with the laboratory observations of Ishihara and Yoshimine (1992). Figure 7 illustrates the match to number of cycles to liquefaction and Figure 8 illustrates stress-strain and stress path behavior produced by the calibrated model when subjected to harmonic loading. The results show the capability of the model to predict response that is consistent with the behavior implied by field observations of the occurrence of liquefaction, and also the phase transformation behavior observed in the field and laboratory. Two one-dimensional models of the IBR014 soil profile were developed – Model S, in which the shallow sandy soils were considered to be susceptible to liquefaction and fully saturated, and Model NS, in which those soils were assumed to be non-susceptible to liquefaction. Aside from the assumed liquefaction susceptibility of the shallow sandy soils, the two profile models were identical.

The results of the site response analyses for both IBR014 models are shown in Figure 9. Ground surface response spectra for Model S are shown in Figure 9(a) along with the geomean spectrum from the IBR014 recorded motion. For this profile, in which the shallow

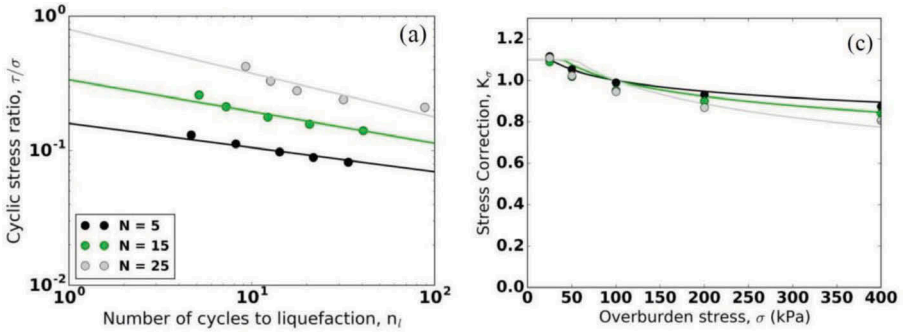

Figure 7. Illustration of consistency of Cocktail Glass model calibration with behavior implied by Boulanger and Idriss (2014) empirical liquefaction triggering model.

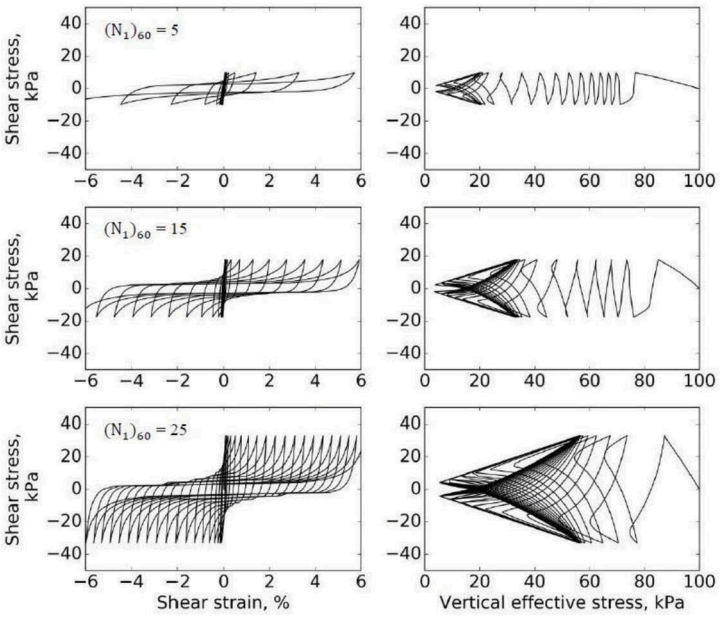

Figure 8. Stress-strain and effective stress path behavior of calibrated Cocktail Glass model at three standard penetration resistances.

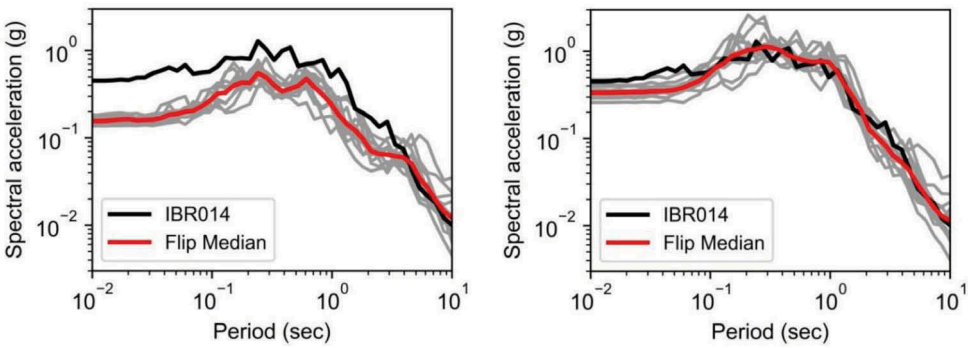

Figure 9. Comparison of response spectra from computed and recorded IBR014 ground surface motions: (a) Model S (shallow soils susceptible), and (b) Model NS (shallow soil non-susceptible).

sandy soils were assumed to be susceptible and fully saturated, the numerical model predicted spectral accelerations that were well below those of the recorded motion at periods below about 5 sec. The reduced low-period response is attributed to early and extensive liquefaction of the shallow

sandy soils, which softened so greatly that higher frequency components of the input motion could not be transmitted to the ground surface. In contrast, the computed spectra for the Model NS profile (Figure 9b), which assumed that the shallow sandy soils were not susceptible to liquefaction, produced ground surface response spectra that were quite consistent with the recorded IBR014 spectrum. Model NS predicted that the layer of medium dense sand at 24-26 m depth, which had the lowest penetration resistance of any sand layers in the profile, liquefied first; other layers of medium dense to dense sand at depths greater than 17 m also liquefied as the strong shaking continued. As a check on the reasonableness of the Model NS

predictions, the intensities of the computed motions at the time of triggering were compared with the intensity of the recorded motion at triggering. In terms of magnitude-corrected PGA, i.e., PGA/MSF where MSF is correlated to number of equivalent loading cycles by the procedure of Liu et al., (2001), the median computed value of 0.34 g (with $\sigma_{\ln IM} = 0.28$) was close to the recorded value of 0.32 g. This provides evidence of the reasonableness of the selected input motions and the non-susceptible soil profile model.

Numerical analyses can also help quantify the CSR and representative penetration resistance values assigned to a particular case history; such data form the basis for empirical prediction of liquefaction potential. Preliminary efforts in this direction have used FLIP to show that a $(N_1)_{60}$ values of 18 in the sand layer at 24-26 m depth produces consistent pore pressure response to that based on the actual, variable penetration resistances for the 11 motions applied to that profile. Total stress analyses produced cyclic stress ratios ranging from 0.34-0.46 depending on the assumed depth of the water table at the time of the Tohoku earthquake. Further studies are underway to refine these preliminary estimated values.

5.3 *Discussion*

The IBR014 record shows clear evidence of rapid and pronounced changes in frequency content that are typical of motions recorded on soil profiles that have liquefied, and surficial evidence of liquefaction was observed in a parking lot near the IBR014 instrument. An initial examination of subsurface conditions could lead to the conclusion that liquefaction of shallow clayey sands took place; however, there are several compelling pieces of evidence that indicate that those soils did not liquefy. Briefly, that evidence includes:

1. Despite the formation of cracks in nearby pavement, surficial evidence of liquefaction was absent at the location of the instrument. Ejecta was observed, however, in a nearby parking lot.
2. Despite the prevalence of the clayey sands in Tsuchiura, they were not observed to liquefy at other sites.
3. High plasticity indices indicated that the clayey sands were clearly not susceptible by one common criterion and borderline non-susceptible by another.
4. Fluctuating groundwater levels at the site suggest that the clayey sand may not have been completely saturated.
5. Low factors of safety obtained from empirical triggering procedures assuming that the shallow sandy soils were liquefiable, combined with their thickness and a thin overlying layer of non-liquefiable soil, suggest that large amounts of ejecta should have been present if those soils had liquefied.
6. Empirical lateral spreading procedures suggest that substantial lateral displacements should have occurred if the shallow sandy soils had liquefied.
7. Advanced numerical modeling shows that liquefaction of the shallow sandy soils would have produced very different ground surface motions than those that were recorded, and that predicted motions were close to the recorded motions in analyses in which liquefaction of those soils was not allowed to occur.

On the other hand, deeper layers of soil at the IBR014 site were non-plastic, medium dense, saturated, and also shown by empirical analyses to have low factors of safety against triggering. These soils were deep enough, and sufficiently interlayered with silty soils, that their liquefaction would not be expected to produce surficial evidence such as sand boils. It would, however, lead to the changes in frequency content that were observed and, by virtue of composition and density, to the dilation-induced acceleration pulses that were also observed in the recorded motions. Finally, advanced nonlinear, effective stress modeling showed that liquefaction of the deeper sand layers produced ground surface motions that were consistent with the recorded motions with liquefaction being triggered at consistent levels of ground motion intensity.

All of this evidence leads to the firm conclusion that liquefaction did occur beneath the IBR014 strong motion station, but it occurred in deep sandy soils some 24-26 m below the ground surface, and not in the sandy soils that exist at shallow depths.

6 SUMMARY AND CONCLUSIONS

Numerical analyses, specifically nonlinear, effective stress ground response analyses, have developed to the point where they can capture the principal aspects of soil behavior under complex earthquake loading conditions. While *a priori* prediction of all details of site response remains quite difficult, such analyses can elucidate the most important mechanisms of response of soils near and well below the ground surface, and can be used to evaluate the sensitivity of site response to various characteristics of soil profiles.

Such analyses require care in characterization of the soil profile, assignment of expected material properties to the various soil units within the profile, and selection of input motions to be used in the analyses. While subsurface characteristics may be available from investigations performed when a strong motion instrument is installed, descriptions of the results of such investigations are often expressed in a relatively crude and simple manner that can obscure significant details of the site's subsurface characteristics. As such, the performance of supplemental subsurface investigations is generally recommended, and can provide the information needed for development of appropriate numerical models. When recorded ground motions at the site of interest are not available, interpolation of nearby recorded motions may be required to estimate the amplitude and spectral characteristics of the motions that produced the motion at the site. Numerical analyses using suites of motions obtained in this manner can elucidate the behavior of the profile, including mechanical and hydraulic interactions between various layers of soil within the profile, and hence help advance understanding of the observed response and reasons for its occurrence.

REFERENCES

Abrahamson, N., Gregor, N. & Addo, K. 2016. BC Hydro ground motion prediction equations for subduction earthquakes. *Earthquake Spectra*, 32(1): 23–44.

Ashford, S. A., Boulanger, R. W., Donahue, J. L., & Stewart, J. P. 2011. Geotechnical quick report on the Kanto plain region during the March 11, 2011 off Pacific coast of Tohoku earthquake, Japan. Geotechnical Extreme Events Reconnaissance (GEER).

Boulanger, R. W. & Idriss, I. M. 2006. Liquefaction susceptibility criteria for silts and clays, *Journal of Geotechnical and Geoenvironmental Engineering*, ASCE, 132(11): 1413–1426.

Bradley, B.A. 2014. Site-specific and spatially-distributed ground-motion intensity estimation in the 2010-2011 Canterbury earthquakes, *Soil Dynamics and Earthquake Engineering*, 61-62: 83–91.

Bray, J.D. & Sancio, R.B. 2006. Assessment of the liquefaction susceptibility of fine-grained soils. *Journal of Geotechnical and Geoenvironmental Engineering*, 132(9): 1165–1177.

FLIP Consortium 2011. FLIP (ver. 7.2.3). August 2011.

Iai,S., Tobita,T., Ozutsumi,O. & Ueda, K. 2011. Dilatancy of granular materials in a strain space multiple mechanism model, *International Journal for Numerical and Analytical Methods in Geomechanics*, 35(3): 360–392.

Iwasaki, T., Tatsuoka, F., Tokida, K., & Yasuda, S., 1978. A practical method for assessing soil liquefaction potential based on case studies at various sites in Japan, *Proceedings*, 2nd International Conference on Microzonation. San Francisco: 885–896.

Kramer, S.L. & Sideras, S.S. & Greenfield, M.W. 2016. The timing of liquefaction and its utility in liquefaction hazard evaluation. *Soil Dynamics and Earthquake Engineering*. 91: 133–146.

Kwak, D.Y., Stewart, J.P., & Brandenberg, S.J. 2015. Spatial correlation of seismic damage for levee systems, *Proceedings*, 6th International Conference on Earthquake Geotechnical Engineering, Christchurch, New Zealand: 1–8.

Liu, A. H., Stewart, J. P., Abrahamson, N. A., & Moriwaki, Y. 2001. Equivalent Number of Uniform Stress Cycles for Soil Liquefaction Analysis, *Journal of Geotechnical and Geoenvironmental Engineering*, ASCE, 127(12): 1017–1026.

Maurer, B.W., Green, R.A., and Taylor, O.-D., S. 2015. Moving towards an improved index for assessing liquefaction hazard: Lessons learned from historical earthquakes, *Soils and Foundations*, 55(4): 778–787.

Stewart, J. P., Kramer, S. L., Kwak, D. Y., Greenfield, M. W., Kayen, R. E., Tokimatsu, J., Bray, D., Beyzaei, C. Z., Cubrinovski, M., Sekiguchi, T., Nakai, S., & Bozorgnia, Y. 2016. PEER-NGL project: open source global database and model development for the Next-Generation of Liquefaction Assessment Procedures, *Soil Dynamics and Earthquake Engineering*, 91: 317–328.

Stockwell, R. G., Mansinha, L., & Lowe., R. P. 1996. Localization of the complex spectrum: The S Transform, *IEEE Trans. Signal Processing*. 44(4): 998–1001.

Van Ballegooy, S., Lacrosse, V., Jacka, M., & Malan, P. 2013. LSN – a new methodology for characterizing the effects of liquefaction in terms of relative land damage severity. Proceedings, 19th NZGS Geotechnical Symposium, Queenstown: 1–8.